

Radiation Heat Transfer in Planar SOFC Components: Application of the Lattice Boltzmann Method

Imen Mejri, Ahmed Mahmoudi, Mohamed A. Abbassi, Ahmed Omri

Abstract—Thermal radiation plays a very important role in the heat transfer combination through the various components of the SOFC fuel cell operating at high temperatures. Lattice Boltzmann method is used for treating conduction-radiation heat transfer in the electrolyte. The thermal radiation heat transfer is coupled to the overall energy conservation equations through the divergence of the local radiative flux. The equation of energy in one dimension is numerically resolved by using the Lattice Boltzmann method. A computing program (FORTRAN) is developed locally for this purpose in order to obtain fields of temperature in every element of the cell. The parameters investigated are: functioning temperature, cell voltages and electrolyte thickness. The results show that the radiation effect increases with increasing the electrolyte thickness, also increases with increasing the functioning temperature and decreases with the increase of the voltage of the cell.

Keywords—SOFC, lattice Boltzmann method, conduction, radiation, planar medium.

I. INTRODUCTION

SOLID oxide fuel cell (SOFC) operates at elevated temperature producing heat which can be used for heating purposes or for feeding gas turbines to produce more power. Fuel cells have been attracting more attention in the search for new efficient and eco-friendly energy sources for future. Because of their high operating temperatures (typically 800–1200 K), thus, radiation heat transfer must be given special consideration in thermal modeling efforts, including stack thermal management and materials development. During the last decades many papers have reported results of numerical calculations, some including the effects of radiation and others not. The methodologies employed vary from highly simplified analysis to much more detailed, computationally expensive methods (often via commercial CFD codes) with sometimes conflicting results and conclusions reported. In [1]-[3], the authors regarded the radiative heat transfer to have a great effect on the heat transfer rate in SOFCs. References [4], [5] investigated the effects of radiative heat transfer in the electrode and the electrolyte layers. Their results revealed that the electrodes can be regarded as optical transparent material, and the radiative heat transfer within the electrodes had a negligible effect on the average cell operating temperature, voltage, or temperature gradients. However, the effects of

radiation heat transfer within the electrolyte depend on the thickness of electrolyte layer, i.e., the thicker the electrolyte layer, the greater the impact of radiative heat transfer. The radiative heat transfer had little influence when the thickness of the electrolyte was less than 15m. The same conclusion was drawn by [6]. The radiative heat transfer with the participating media in SOFCs was investigated in detail by [7]. Because of the low emissivity of the gas and the small channel sizes, the gas was optically thin, and the effect of participating media on thermal radiation was minimal in the planar geometry, but it was likely to be significant in the tubular geometry. Reference [8] also investigated the radiative heat transfer with participating media in the anode and they found it had little influence on the performance of SOFCs under the ordinary operation conditions. They also indicated that the surface-to-surface thermal radiation in the flow channels had great effects on the SOFCs. Reference [9] numerically investigated the effects of surface-to-surface thermal radiation on the performance of planar SOFCs, and revealed that the temperature distribution in the cell became flat as the radiative heat exchange inside the channels was considered. The radiative heat transfer has received much more attention in recent years [10]-[13]. Based on a Monte Carlo Ray Tracing method, a numerical methodology aimed to predict the thermal radiation of materials used in the cell design with a planar geometry was developed in [10]. Reference [11] developed a relatively simple model to rapidly evaluate various configurations and operating conditions for tubular anode-supported SOFC stacks, and they concluded that the radiative heat transfer is remarkably effective at removing the heat from tube bundles of the stack. A surface-to-surface radiation model was employed in [12] to analyze the influence of different operating conditions on the temperature distribution in the anode supported tubular cell. A mathematical evaluation of view factors for radiative heat exchange in longitudinally distributed SOFC modeling was introduced by [13]. The detailed radiation model based on analytical view factors predicted more uniform distribution of the cell temperature and current density in the overall SOFC modeling. Nevertheless, most of the existing heat transfer models for the SOFCs simply ignored the effect of thermal radiation [14], even though this effect is important when the cell operating temperature is higher than 800 K [2].

The present work studies the radiation effect within the solid anode, electrolyte, and cathode SOFC layers. Although it may seem unlikely that radiation could be important within these solid ceramic layers, this is in fact not an unreasonable hypothesis given the high temperatures involved and the

Imen Mejri is with Unité de Recherche Matériaux, Energie et Energies Renouvelables (MEER), Faculté des Sciences de Gafsa, B.P.19, Zarroug, Gafsa, 2112, Tunisie (Corresponding author; e-mail: im.mejri85@yahoo.fr).

Ahmed Mahmoudi, Mohamed A. Abbassi, and Ahmed Omri are with Unité de Recherche Matériaux, Energie et Energies Renouvelables (MEER), Faculté des Sciences de Gafsa, B.P.19, Zarroug, Gafsa, 2112, Tunisie (e-mail: ahmed.mahmoudi@yahoo.fr, abbassima@gmail.com ahom206@yahoo.fr).

thickness of the electrode and electrolyte layers. The study is performed for two functioning temperature values (870K and 1073K), two cell voltage values (0.5V and 0.7V) and for several values of the electrolyte thickness (5-30 μ m). In addition to the radiation source, only the Joule effect is considered as a heat source. Lattice Boltzmann method is used to solve conduction-radiation equation in SOFC planar geometry.

II. MATHEMATICAL FORMULATION

A. Problem Statement

In general, the electrolyte and the porous electrodes of SOFCs are semitransparent materials; that is, they can absorb, scatter, and emit thermal radiation. The energy equation is:

$$\rho c_p \frac{\partial T}{\partial t} = k \nabla^2 T - \vec{\nabla} \cdot \vec{q}_R + S_{\text{Ohm}} \quad (1)$$

where ρ is the density, c_p is the specific heat, k is the thermal conductivity, \vec{q}_R is the radiative heat flux and S_{Ohm} is the heat source by Joule effect.

B. Lattice Boltzmann Simulation: Energy Equation

For a one-dimensional planar geometry, in the LBM with a D1Q2 lattice, the discrete Boltzmann equation with Bhatnagar- Gross-Krook (BGK) approximation is given by [15]:

$$\frac{\partial f_i(\vec{x}, t)}{\partial t} + \vec{e}_i \cdot \nabla f_i(\vec{x}, t) = -\frac{1}{\tau} [f_i(\vec{x}, t) - f_i^{eq}(\vec{x}, t)] \quad i = 1 \text{ and } 2 \quad (2)$$

where f_i is the particle distribution function denoting the number of particles at the lattice node \vec{x} and time t moving in direction i with velocity \vec{e}_i along the lattice $\Delta x = e_i \Delta t$ connecting the neighbors, τ is the relaxation time, and f_i^{eq} is the equilibrium distribution function. The relaxation time τ for the D1Q2 lattice is computed from:

$$\tau = \frac{\alpha}{|\vec{e}_i|^2} + \frac{\Delta t}{2} \quad (3)$$

where α is the thermal diffusivity. For this lattice, the two velocities e_1 and e_2 , and their corresponding weights w_1 and w_2 , are given by:

$$e_1 = \frac{\Delta x}{\Delta t} \quad e_2 = -\frac{\Delta x}{\Delta t} \quad (4)$$

$$w_1 = w_2 = \frac{1}{2} \quad (5)$$

After discretization, (2) is written as:

$$f_i(\vec{x} + \vec{e}_i \Delta t, t + \Delta t) = f_i(\vec{x}, t) - \frac{1}{\tau} [f_i(\vec{x}, t) - f_i^{eq}(\vec{x}, t)] \quad (6)$$

The temperature is obtained after summing f_i over all direction:

$$T(\vec{x}, t) = \sum_{i=1,2} f_i(\vec{x}, t) \quad (7)$$

To process (6), an equilibrium distribution function is required, which for a conduction-radiation problem is given by:

$$f_i^{eq}(\vec{x}, t) = w_i T(\vec{x}, t) \quad (8)$$

To account for the volumetric radiation, the energy equation in the LBM formulation, (6) is modified to [16]:

$$f_i(\vec{x} + \vec{e}_i \Delta t, t + \Delta t) = f_i(\vec{x}, t) - \frac{1}{\tau} [f_i(\vec{x}, t) - f_i^{eq}(\vec{x}, t)] - \frac{\Delta t w_i}{\rho c_p} \left(\frac{\partial q_R}{\partial x} - S_{\text{Ohm}} \right) \quad (9)$$

where the divergence of radiative heat flux $\frac{\partial q_R}{\partial x}$ is given by:

$$\frac{\partial q_R}{\partial x} = \beta(1-\omega)(4\pi \frac{\sigma_B T^4}{\pi} - G) \quad (10)$$

The heat source by Joule effect is given by the following expression:

$$S_{\text{Ohm}} = \frac{j^2}{\sigma} \quad (11)$$

G is the incident radiation, β is the extinction coefficient, ω the scattering albedo, j is the current density, σ is the ionic/electronic conductivity.

C. Lattice Boltzmann Simulation: Radiative Equation

The experimental data [17] suggest that SOFC electrodes are opaque and, therefore, volumetric radiation can be neglected or treated in the limit of the optically thick media approximation, for which the optical distance $\tau_L = \beta L \gg 1$, if the extinction coefficient is known, in this case, the very simple, Rosseland approximation can be invoked. for the studied problem the volumetric radiation is neglected in the electrodes. On the other hand, the electrolyte appears to be optically thin [17] $\tau_L = \beta L \leq 1$, and can be considered an isotropic, non-diffusing gray medium [2] $\beta = 500 \text{ m}^{-1}$ and

$\omega = 0$), in the case of a 1D, plane-parallel medium, the lattice Boltzmann method can be used to solve the radiative energy equation (RTE):

$$\frac{1}{c} \frac{\partial I(\vec{x}, \vec{s}, t)}{\partial t} + \frac{\partial I(\vec{x}, \vec{s}, t)}{\partial s} = -\beta I(\vec{x}, \vec{s}, t) + \beta(1-\omega)I_b(\vec{x}, t) + \frac{\beta\omega}{4\pi} \int_{\Omega'=4\pi} I(\vec{x}, \vec{s}', t) p(\vec{s}' \rightarrow \vec{s}) d\Omega' \quad (12)$$

where c is the speed of light in the medium, S is the energy transport direction, $I_b = \sigma_B T^4 / \pi$ is the Planck's black body intensity, $d\Omega$ is the solid angle and $p(s' \rightarrow s)$ the anisotropic scattering phase function (for the studied problem $p(s' \rightarrow s) = 1$). Equation (12) can be recast as:

$$\frac{1}{c} \frac{\partial I(\vec{x}, \vec{s}, t)}{\partial t} + \vec{s} \cdot \nabla I(\vec{x}, \vec{s}, t) = -\beta I(\vec{x}, \vec{s}, t) + \beta S_R(\vec{x}, \vec{s}, t) \quad (13)$$

where S_R is the radiative source term given as:

$$S_R(\vec{x}, \vec{s}, t) = (1-\omega)I_b(\vec{x}, t) + \frac{\omega}{4\pi} \int_{\Omega=4\pi} I(\vec{x}, \vec{s}', t) d\Omega' \quad (14)$$

The radiative boundary condition for (11), when the wall bounding the physical domain is assumed grey and emits and reflects diffusely, can be expressed as

$$I(\vec{x}_E, \vec{s}) = \epsilon_E I_b(\vec{x}_E) + \frac{(1-\epsilon_E)}{\pi} \int_{\Omega=2\pi} [I(\vec{x}_E, \vec{s}') |\vec{n} \cdot \vec{s}'|]_{\vec{n} \cdot \vec{s}' > 0} d\Omega' \quad (15)$$

$$I(\vec{x}_W, \vec{s}) = \epsilon_W I_b(\vec{x}_W) + \frac{(1-\epsilon_W)}{\pi} \int_{\Omega=2\pi} [I(\vec{x}_W, \vec{s}') |\vec{n} \cdot \vec{s}'|]_{\vec{n} \cdot \vec{s}' < 0} d\Omega' \quad (16)$$

ϵ_W and ϵ_E emissivities of the west and the east boundaries.

$$S_R(\vec{x}, \vec{s}, t) = (1-\omega)I_b(\vec{x}, t) + \frac{\omega}{4\pi} G(\vec{x}, t) \quad (17)$$

Multiplying (13) throughout by the speed of light c , the radiative transfer equation along any lattice link designated by the index i can be written as:

$$\frac{DI_i}{Dt}(\vec{x}, \vec{s}, t) = \frac{\partial I_i}{\partial t} + \vec{c} \cdot \nabla I_i = -c\beta(I_i - S_i) \quad i=1, \dots, M \quad (18)$$

Let \vec{e}_i be the velocity of propagation along the i th lattice link of the DIQM lattice structure. If the velocity of light \vec{c} is fictitiously made equal to the velocity of particle propagation

in the LBM, $\vec{c} = \vec{e}$ a convenient tool would be obtained to solve the radiative transfer equation using the LBM approach

$$\frac{\partial I_i}{\partial t} + \vec{e}_i \cdot \nabla I_i = e_i \beta (S_i - I_i) \quad i=1, \dots, M \quad (19)$$

Discretizing (19), we obtain:

$$I_i(\vec{x} + \vec{e}_i \Delta t, t + \Delta t) = I_i(\vec{x}, t) + \Delta t e_i \beta (S_i - I_i) \quad i=1, \dots, M \quad (20)$$

Clearly in (20), the term on the right hand side can be seen as the collision term in the LBM, where I_i is the intensity particle distribution function. Using the standard LBM terminology, (12) can be written as:

$$I_i(\vec{x} + \vec{e}_i \Delta t, t + \Delta t) = I_i(\vec{x}, t) + \frac{\Delta t}{\tau_R} [I_i^{eq}(\vec{x}, t) - I_i(\vec{x}, t)] \quad (21)$$

where τ_R is the relaxation time for the collision process and I_i^{eq} is the equilibrium particle distribution function.

$$\tau_R = \frac{1}{e_i \beta} \quad \text{and} \quad I_i^{eq} = S_{Ri} \quad (22)$$

In (10), G is the irradiation and \vec{q}_R is the heat flux due to diffuse radiation, are computed from the following:

$$G = 4\pi \sum_{i=1, M} I_i \sin \gamma_i \sin\left(\frac{\Delta \gamma_i}{2}\right) \quad (23)$$

$$q_R = 2\pi \sum_{i=1, M} I_i \sin \gamma_i \cos \gamma_i \sin(\Delta \gamma_i) \quad (24)$$

γ is the polar angle.

D. Ohmic Source Expression

The Ohmic source is caused by Joule effect in the three components of SOFC: Cathode, Electrolyte and Anode. The heat source by Joule effect is given by the following expression:

$$S_{Ohmi} = \frac{j^2}{\sigma_i} \quad (25)$$

i : anode, cathode and electrolyte.

The current density for several cell voltages imposed, is given by:

$$j = \frac{U - E_{Nernst}}{R_{Ohm}} \quad (26)$$

$$R_{Ohm} = \frac{e_{an}}{\sigma_{an}} + \frac{e_{ca}}{\sigma_{ca}} + \frac{e_{el}}{\sigma_{el}} \quad (27)$$

where R_{Ohm} is the Ohmic resistance, U is the cell voltage and E_{Nernst} is the Nernst potential. The parameters values (electrical/ionic conductivity, thermal conductivity, the electrode and electrolyte thickness and the Nernst potential) are given in Tables I and II.

III. VALIDATION OF THE NUMERICAL CODE

In order to check on the accuracy of the numerical technique employed for the solution of the considered problem, the present numerical code was validated with the published study of [18] is represented in Fig. 1 (a)-(c), for all results presented in Fig. 1, the boundaries are black. Fig. 1 (a) shows the effect of the extinction coefficient by comparing the results obtained by the LBM and the published results, for $\omega=0.0$ and $N=0.1$. These comparisons are shown for $\beta = 0.1, 1.0$ and 2.0 . In fig.1b, for $\beta = 1.0$ and $N = 0.01$, these comparisons are made for $\omega=0.1, 0.5$ and 0.9 . In fig.1c, for $\beta = 1.0$ and $\omega=0.0$, these comparisons are made for $N = 0.01, 0.1$ and 1.0 . It can be seen that in all cases, found results are in good agreement with those published.

IV. RESULTS AND DISCUSSION

The heat distribution is studied as a function of several parameters such as the operating temperature, cell voltages and electrolyte thickness; the effects of these parameters, in the absence and presence of the radiation, are shown in the temperature distribution and the maximum temperature.

Figs. 2 (a), (b) show the temperature distribution in the absence and presence of the effect of the radiation for two cell voltages (0.5V and 0.7V) and for two operating temperatures (873K and 1073K). In the absence of the radiation effect, the results are compared with the published results [19]; good precision is found which shows the efficiency of the LBM. For both cell voltages and for both operating temperatures, the radiation effect reduces the temperature in the medium.

Table III presents the maximum value of temperature in the presence and in the absence of the radiation effect, and the difference between them. It is shown that the temperature

difference is small and can be neglected for the electrolyte thickness equal to $15\mu\text{m}$.

Table IV presents the maximum value of temperature in the presence and in the absence of the radiation effect, and the difference between them, for two cell voltages (0.5V and 0.7V), for two operating temperatures (873K and 1073K) and for several electrolyte thickness. The results obtained in Table IV are shown in Fig. 3 which shows the radiative effect as function of the electrolyte thickness. It is observed that the radiative effect increases with the increase of the operating temperature and decreases with the increase of the cell voltage. The radiative effect increases with the increase of the electrolyte thickness, higher temperature differences are obtained for the electrolyte thicknesses higher to $15\mu\text{m}$.

V. CONCLUSION

Combined conduction–radiation problem in one-dimensional gray planar absorbing, emitting and anisotropically scattering medium has been investigated by the LBM. The LBM is used for modeling the radiation effect in the various components of the SOFC fuel cell operating at high temperatures. The results show that the radiation effect increases with the increase of the electrolyte thickness for higher thickness to $15\mu\text{m}$, the effect of radiation becomes important. Also, radiation effect depends on the operating temperature, the radiative effect increases with the increase of the operating temperature. Also, the cell voltage influences the radiative effect, It is observed that the radiative effect decreases with the increase of the cell voltage.

TABLE I
THE PARAMETERS VALUES OF SOFC COMPONENTS [19]

	cathode	electrolyte	anode
Conductivity k [W/(m·K)]	2.0	2.0	2.0
thickness (μm)	300.0	15.0	20.0
σ (S/cm)	127.92	0.14	303.15

TABLE II
VALUES OF THE NERNST VOLTAGE [19]

	E_{Nernst} (V)
T=873K	1.109
T=1073K	1.055

TABLE III

RADIATION EFFECT FOR AN ELECTROLYTE THICKNESS EQUAL TO 15 μm , FOR TWO VALUES OF OPERATING TEMPERATURES ($T=873\text{K}-1073\text{K}$) AND FOR TWO CELL VOLTAGES ($U=0.5\text{V}-0.7\text{V}$)

		U=0.5V	U=0.7V
T=873K			
T_{max}	Without radiation	873.60	873.28
	With radiation	873.45	873.17
ΔT_{max}		0.15	0.11
T=1073K			
T_{max}	Without radiation	1076.02	1074.32
	With radiation	1075.21	1073.89
ΔT_{max}		0.81	0.43

TABLE IV

RADIATION EFFECT DEPENDING ON THE ELECTROLYTE THICKNESS FOR TWO VALUES OF OPERATING TEMPERATURES ($T=873\text{K}-1073\text{K}$) AND FOR TWO CELL VOLTAGES ($U=0.5\text{V}-0.7\text{V}$)

Electrolyte thickness of SOFC (μm)	5	10	15	20	25	30
U=0.5V T=1073K						
T_{max} (K) (Without radiation)	1073.79	1074.79	1076.02	1077.47	1079.17	1081.13
T_{max} (K) (With radiation)	1073.68	1074.43	1075.21	1076.00	1076.80	1077.58
ΔT_{max}	0.11	0.36	0.81	1.47	2.37	3.55
U=0.7V T=1073K						
T_{max} (K) (Without radiation)	1073.34	1073.79	1074.32	1074.96	1075.71	1076.57
T_{max} (K) (With radiation)	1073.27	1073.57	1073.89	1074.21	1074.54	1074.87
ΔT_{max}	0.07	0.22	0.43	0.75	1.17	1.70
U=0.5V T=873K						
T_{max} (K) (Without radiation)	873.15	873.35	873.60	873.89	874.23	874.62
T_{max} (K) (With radiation)	873.13	873.28	873.45	873.64	873.84	874.05
ΔT_{max}	0.02	0.07	0.15	0.25	0.39	0.57
U=0.7V T=873K						
T_{max} (K) (Without radiation)	873.07	873.16	873.28	873.41	873.57	873.75
T_{max} (K) (With radiation)	873.04	873.10	873.17	873.24	873.32	873.41
ΔT_{max}	0.03	0.06	0.11	0.17	0.25	0.34

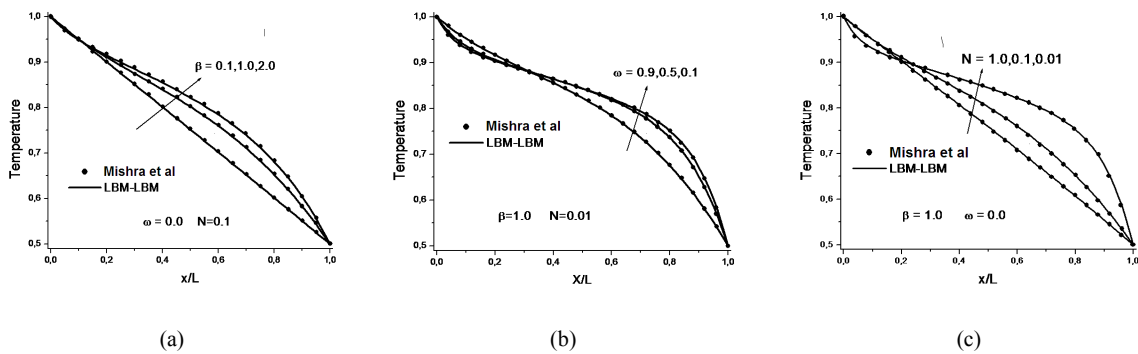


Fig. 1 Comparison of non dimensional temperature in a planar medium at the steady-state for the effects of (a) extinction coefficient, (b) scattering albedo and (c) conduction–radiation parameter

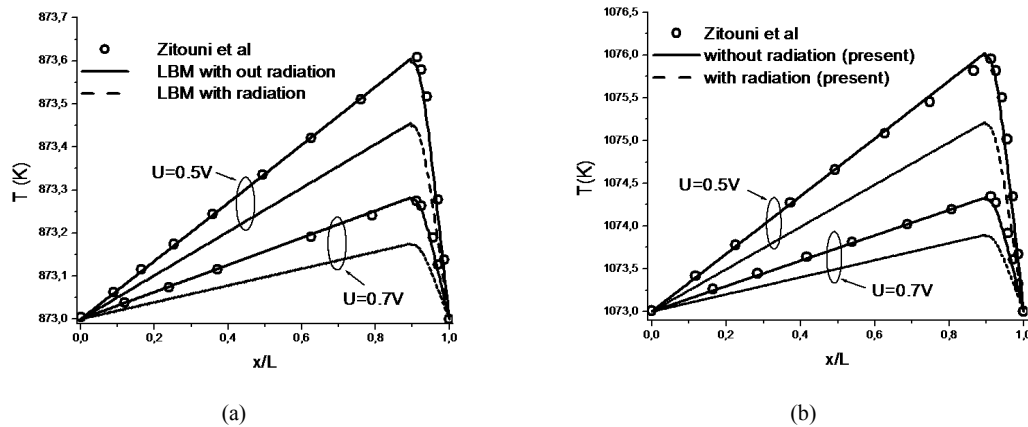


Fig. 2 Comparison of the temperature distribution with and without radiation effect depending on the cell voltage for (a) $T=873\text{K}$ and (b) $T=1073\text{K}$

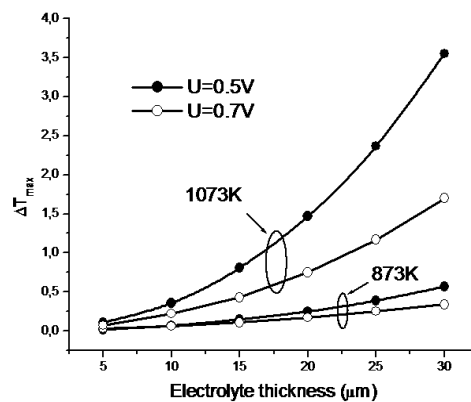


Fig. 3 Radiation effect depending on the electrolyte thickness for $T=873\text{K}$ - 1073K and for $U=0.5\text{V}$ - 0.7V

REFERENCES

- [1] H. Karoliussen, K. Nisancioglu and A. Solheim, "Use of effective conductivities and unit cell-based supraelements in the numerical simulation of solid oxide fuel cell stacks" *J. Appl. Electrochem*, vol.28, pp.283–288, 1998.
- [2] S. Murthy and A.G. Fedorov, "Radiation heat transfer analysis of the monolith type solid oxide fuel cell", *J. Power Sources*, vol.124, pp.453–458, 2003.
- [3] G. Brus and J.S. Szmyd, "Numerical modelling of radiative heat transfer in an internal indirect reforming-type SOFC", *J. Power Sources*, vol.181, pp.8–16, 2008.
- [4] D.L. Damm and A.G. Fedorov, "Spectral radiative heat transfer analysis of the planar SOFC" *J. Fuel Cell Sci. Technol*, vol.2, no.4, pp.258–262, 2005.
- [5] D.L. Damm and A.G. Fedorov, "Radiation heat transfer in SOFC materials and components" *J. Power Sources*, vol.143, no.1, pp.158–165, 2005.
- [6] K.J. Daun, S.B. Beale and F. Liu, "Radiation heat transfer in planar SOFC electrolytes" *J. Power Sources*, vol.157, pp.302–310, 2006.
- [7] J.D.J. VanderSteen and J.G. Pharoah "Modeling radiation heat transfer with participating media in solid oxide fuel cells" *J. Fuel Cell Sci. Technol*, vol.3, pp.62–67, 2006.
- [8] D. Sanchez, R.Chacartegui and A. Munoz "Thermal and electrochemical model of internal reforming solid oxide fuel cells with tubular geometry" *J. Power Sources*, vol.160, pp.1074–1087, 2006.
- [9] H. Yakabe, T. Ogiwara, M. Hishinuma and I.Yasuda "3-D model calculation for planar SOFC" *J. Power Sources*, vol.102, pp.144–154, 2001.
- [10] B. Rousseau, H. Gomart, D.S.M. Domingos, E. Patrick, R. Mathilde, D. Romain and L. Pascal "Modelling of the radiative properties of an opaque porous ceramic layer", *J. Electroceram*, vol.27, pp.89–92, 2011.
- [11] R.J. Kee, B.L. Kee and J.L. Martin "Radiative and convective heat transport within tubular solid-oxide fuel-cell stacks" *J. Power Sources*, vol.195, pp.6688–6698, 2010.
- [12] M. Garcia-Camprubi, H. Jasak and N. Fueyo, "CFD analysis of cooling effects in H_2 -fed solid oxide fuel cells" *J. Power Sources*, vol.196, pp.7290–7301, 2011.
- [13] C. Bao, N. Cai and E.Croiset, "An analytical model of view factors for radiation heat transfer in planar and tubular solid oxide fuel cells" *J. Power Sources*, vol.196, pp.3223–3232, 2011.
- [14] T.X. Ho, P. Kosinski and A.C. Hoffmann, "Effects of heat sources on the performance of a planar solid oxide fuel cell" *Int. J. Hydrogen Energy*, vol.35, pp.4276–4284, 2010.
- [15] S. Succi, "The Lattice Boltzmann Equation for Fluid Dynamics and Beyond", *Oxford University Press*, New York, 2001.
- [16] SC. Mishra and A.Lankadasu, "Analysis of Transient Conduction and Radiation Heat Transfer Using the Lattice Boltzmann Method and the Discrete Transfer Method", *Numer. Heat Transfer A*, vol.47, pp.935–54, 2005.
- [17] D.L. Damm and A.G. Fedorov, Proc. ASME Int. Mech. Eng. Congress Expo. Anaheim, CA, 2004.
- [18] SC. Mishra, P. Talukdar, D. Trimis and F. Durst, "Computational efficiency improvements of the radiative transfer problems with or without conduction-a comparison of the collapsed dimension method and the discrete transfer method", *Int J of Heat and Mass Transfer*, vol.46, pp.3083–95, 2003.
- [19] B. Zitouni, H. Ben Moussa and K. Oulmi, "Studying on the increasing temperature in IT-SOFC: Effect of heat sources", *Journal of Zhejiang university science A*, vol.8, pp.1500-1504, 2007.